International Journal of Engineering Research & Management Technology
ISSN: 2348-4039
Volume 9, Issue-4 July-August- 2022
Email: editor@ijermt.org www.ijermt.org

USAGE OF WET CHEMICAL METHOD IN THE CHARACTERIZATION OF NANO FERRITES

Shiksha Hooda
Research Scholar in Kalinga University

Abstract

For the purpose of this investigation, a wet chemical co-precipitation approach was utilised for the production of pure and doped nickel ferrite nanoparticles at a low temperature. The content of nickel ranged from 2% to 8% during the course of the experiment. The Fourier transform infrared spectrometer, ultra-violet visible spectroscopy, scanning electron microscopy, and powder X-ray diffraction are the instruments that are used to characterise the structural properties of the material, as well as the optical absorption and transmission, surface morphology, and surface properties of the material. It has been discovered that an increase in the quantity of nickel results in an increase in the band gap energy, as well as a transmission and size increase. The increase in size of the nickel ferrite is related with a red shift of the peaks that can be seen in the UV–visible spectra. It is possible to utilise it to manufacture devices that are meant to store data, as well as for the categorization of inorganic materials, which plays a very essential part in the many elements of life owing to the exceptional magnetic, electrical, and optical capabilities that they possess.

keywords: *wet chemical, nano Ferrites, chemical*

INTRODUCTION

The purpose, combination, and characterisation of nanophase materials are all topics of active study that are being conducted right now. The study of numerous spineltype ferrites is being done in terms of the synthesis of their nanoparticles at room temperatures using a variety of different methods, in terms of the potential applications of these nanosized magnetic materials in particular technological areas, and also in terms of the study of the magnetic properties of the nanoferrite materials. For a range of applications, including targeted medication administration, ferrofluids, medical imaging and other biomedical applications, magnetic data storage, etc., nanosized ferrites with a homogeneous and narrow particle size distribution are needed. Ferrite materials are characterised by a powerful ferromagnetic characteristic, the nature of which is determined by the electronic configuration of the atoms that make up the substances. Therefore, in order to characterise the magnetic behaviour of the ferrite structure, it is vital to have a solid knowledge of the electronic state of the elements that are present in the ferrite structure. Due to the intriguing features of spinel ferrites, such as their high resistivity, mechanical hardness, substantial stability, and potentially useful memory store capacity, these minerals have been the subject of much research. When compared to their bulk counterparts, the characteristics of nanosized ferrites in magnetic media are completely different from those of their bulk counterparts. Copper ferrites are of the utmost importance, not only for practical applications but also for the theoretical comprehension of all spinel ferrites. In the past, powdered forms of copper ferrite were subjected to a substantial amount of research. Because of its large surface area, copper ferrite is highly valued for use in catalytic applications. In most cases, increased surface areas are accompanied by decreased particle sizes. As a result, the manufacture of copper ferrite particles on the nanoscale will be an interesting topic to research. 20 Nickel ferrite is a kind

of soft ferrite that has a high electrical resistivity and a low magnetic coercivity. This ferrite is an ideal choice for the core material of power transformers used in electronic and telecommunications applications due to its high electrical resistivity as well as its superb magnetic characteristics. Because of its strong coercivity and relatively considerable crystal anisotropy, barium ferrite is recognised as a prominent example of a permanent magnetic material. Nevertheless, it is also a prominent candidate material for use in the development of improved magnetic recording media. Wet chemical procedures allow for the synthesis of nanoparticles that can have their sizes and characteristics precisely regulated.

Material and Method

Synthesis of Pure Magnetic Ferrite Nanoparticles

The wet chemical coprecipitation approach was utilised in the production of magnetic nanoparticles. Ferric chloride ($FeCl_3 \cdot 6H_2O$) is the precursor that is utilised during the manufacture of pure ferrite nanoparticles. Sodium hydroxide is utilised as the precipitating agent throughout this process. When washing the precipitates, ethanol (C_2H_6O) and distilled water are the two most common solvents utilised. Ferric chloride ($FeCl_3 \cdot 6H_2O$) was measured at 3.244 grammes (0.4 M) in a glass beaker with a volume of 50 millilitres, and sodium hydroxide (NaOH) was measured at 2.99 grammes (3 M) in a glass beaker with a volume of 25 millilitres. This is a schematic diagram for the synthesis of pure ferrite nanoparticles. While maintaining a temperature of 80 degrees Celsius and using a magnetic stirrer to maintain a steady stir, sodium hydroxide was slowly added to the solution of ferric chloride over the course of forty minutes. It is necessary for the solution's pH to be more than 12. The produced precipitate should be filtered through filter paper before being dried in an oven at a constant temperature overnight. After being dried, the precipitates were annealed at a temperature of 600 degrees Celsius for six hours. The result is nanoparticles made entirely of magnetic ferrite (Fig. 1).

Synthesis of Nickel Ferrite Nanoparticles

Wet chemical co-precipitation was used in the production of magnetic nickel ferrite nanoparticles. This method yielded the same results as the previous one. Ferric chloride ($FeCl_3 \cdot 6H_2O$), nickel chloride ($NiCl_2 \cdot 6H_2O$), and sodium hydroxide (NaOH), which is utilised as a precipitating agent, are the precursors that are required for the manufacture of nickel ferrite nanoparticles. When washing the precipitates, ethanol (C_2H_6O) and distilled water are the two most common solvents utilised. Different concentrations of nickel ferrite nanoparticles are produced throughout the synthesis process.

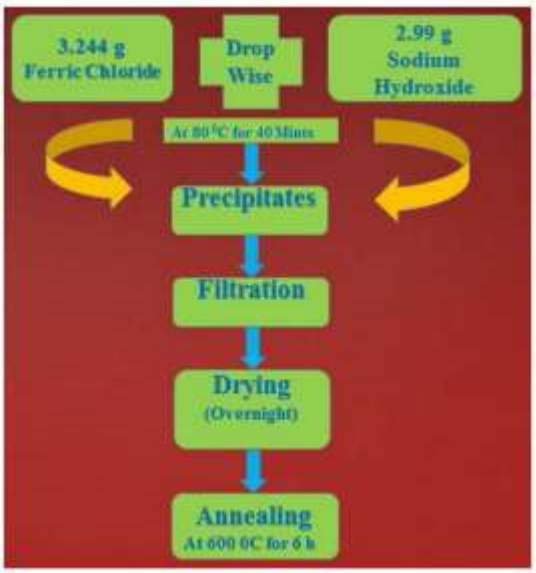

Fig. 1 Schematic diagram for the synthesis of pure ferrite nanoparticles

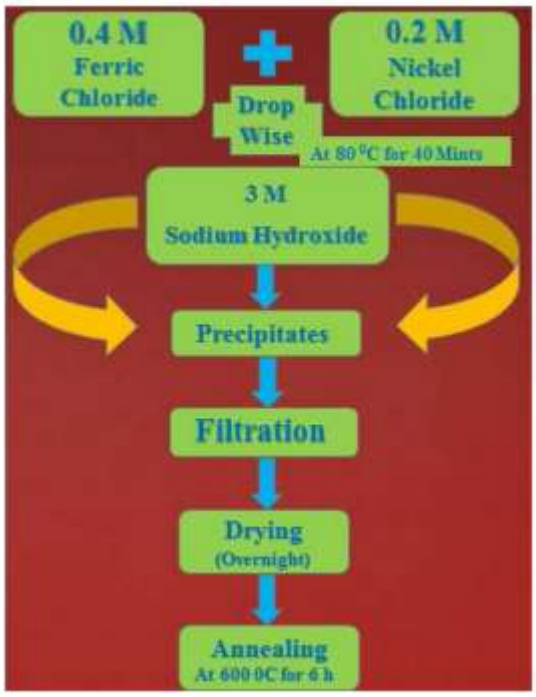

Fig. 2 Schematic diagram for the synthesis of nickel ferrite nanoparticles

in magnetic ferrite nanoparticles, the nickel content was 2, 4, 6, and 8% respectively. Ferric chloride (FeCl3•6H2O) and nickel chloride (NiCl2•6H2O) were measured in a 50 ml glass beaker during the synthesis of nickel ferrite nanoparticles, while 2.99 g (3 M) of sodium hydroxide (NaOH) was measured in a 25 ml beaker. The schematic diagram for the synthesis of nickel ferrite nanoparticles is shown in Figure 2. In order to obtain the several varieties of nickel ferrite nanoparticles, certain amounts of the precursors are required. Various masses of nickel ferrite, such as 0.025, 0.0259, 0.077, and 0.0103 g, as well as ferric chloride, such as 3.18, 3.114, 3.05, and 2.98 g, are utilised to produce 2, 4, 6, and 8% nickel ferrite nanoparticles, respectively. The solution of ferric chloride and nickel chloride was heated to a constant temperature of 80 degrees Celsius for forty minutes while the magnetic stirrer indicated in figure 3a was continuously stirred. The sodium hydroxide was added to the solution drop by drop. It is necessary for the

solution's pH to be more than 12. The produced precipitate should be filtered through filter paper before being dried in an oven at a constant temperature overnight. The precipitates were then annealed at a temperature of 600 degrees Celsius for a period of six hours. After this, we obtain magnetic nickel ferrite nanoparticles with varying concentrations of nickel in each particle. Figure 3 depicts the experimental setup as well as the procedures that must be taken in order to successfully finish the synthesis of pure ferrite as well as nickel ferrite nanoparticles in the laboratory.

Characterizations

Powder X-ray diffraction (XRD), scanning electron microscopy (SEM), ultra-violet visible spectroscopy (UV–Vis), and a Fourier-transform infrared spectrometer were utilised in order to carry out the characterization of the generated magnetic samples (FTIR). X-ray powder diffraction (XRD) was performed with a source of copper Cu-k, at a wavelength of 1.5406, at a voltage of 60 kV and a current of 30 mA, in order to investigate the crystal structural characteristics, grain size, and phase identification. After the samples had been processed, they were placed in diffractometers, which then began running and collecting data continually. The formula developed by Debye and Scherrer, which may be found in equation 1, is used to determine the size of the nanoparticles.

$$D = \frac{0.9\lambda}{\beta \cos\theta} \qquad (1)$$

where, λ is the wave length of X-ray used which is 1.5406 Å [22]. β is the full width of half maxima of the peak. θ is the angle of diffraction for X-rays when applied to the planes hkl. The characterisation instrument known as scanning electron microscopy (SEM) is able to provide information regarding the sample's size as well as its morphology. This is accomplished by the imaging of the sample at a variety of resolutions. In this study, imaging is taken using a scanning electron microscope (SEM) with a resolution of fifty micrometres, and an analysis is performed on the varying particle sizes of pure ferrite and nickel ferrite at a variety of concentrations. The SEM equipment has been used to characterise these materials with an applied voltage of 15 kV. The scanning electron microscope gives us information on the size range of the nanoparticles. In this work, the optical characteristics of the material that was synthesised using the co-precipitation process were investigated using a method known as ultra-violet visible spectroscopy, abbreviated as UV–Vis. This covers the examination of the absorbance of the produced nanoparticles with varying concentrations of nickel, which corresponds to the wavelength of the ultra-violet and visible light spanning from 200 to 500 nm, and the absorption range is 0–0.15. Because the wavelength of the light travels down the horizontal axis (Y-axis), and the absorbance of the material travels along the vertical axis, the relationship between the two should be straightforward (X-axis). The Fourier-transform infrared spectrometer, often known as FTIR, is an instrument that analyses the transmittance of nanoparticles when they are subjected to the effect of infrared light (IR)

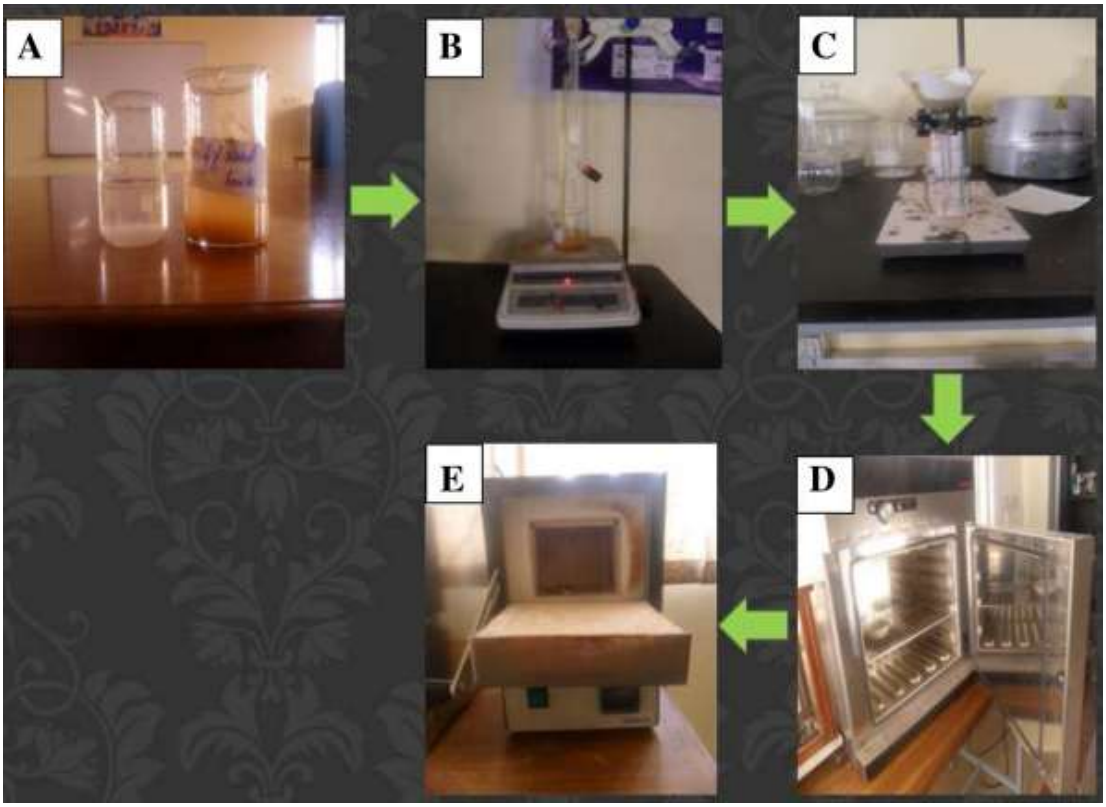

Fig. 3 Experimental setup. a Solution, b drop wise addition of sodium hydroxide, c filtration, d drying, e annealing.

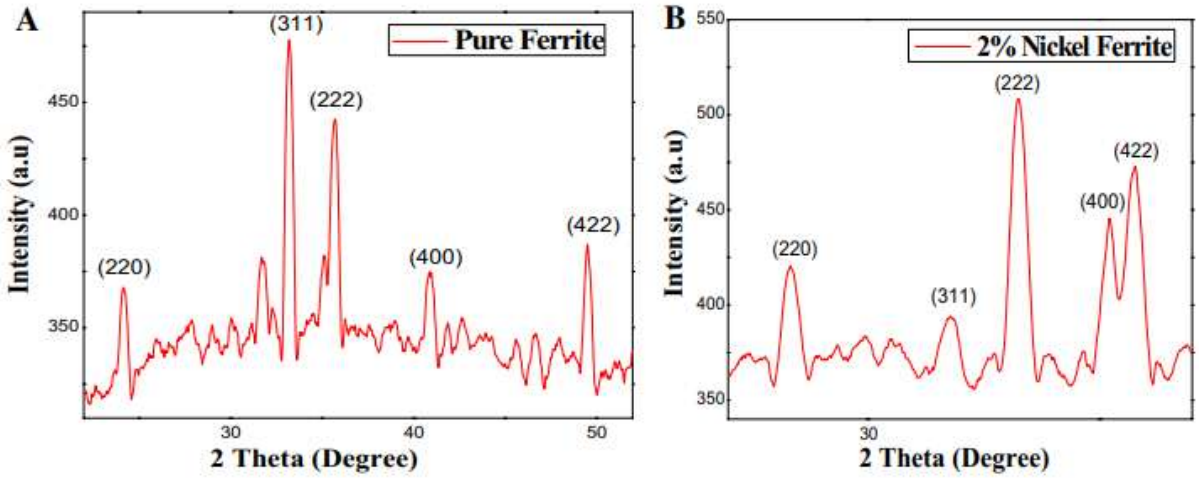

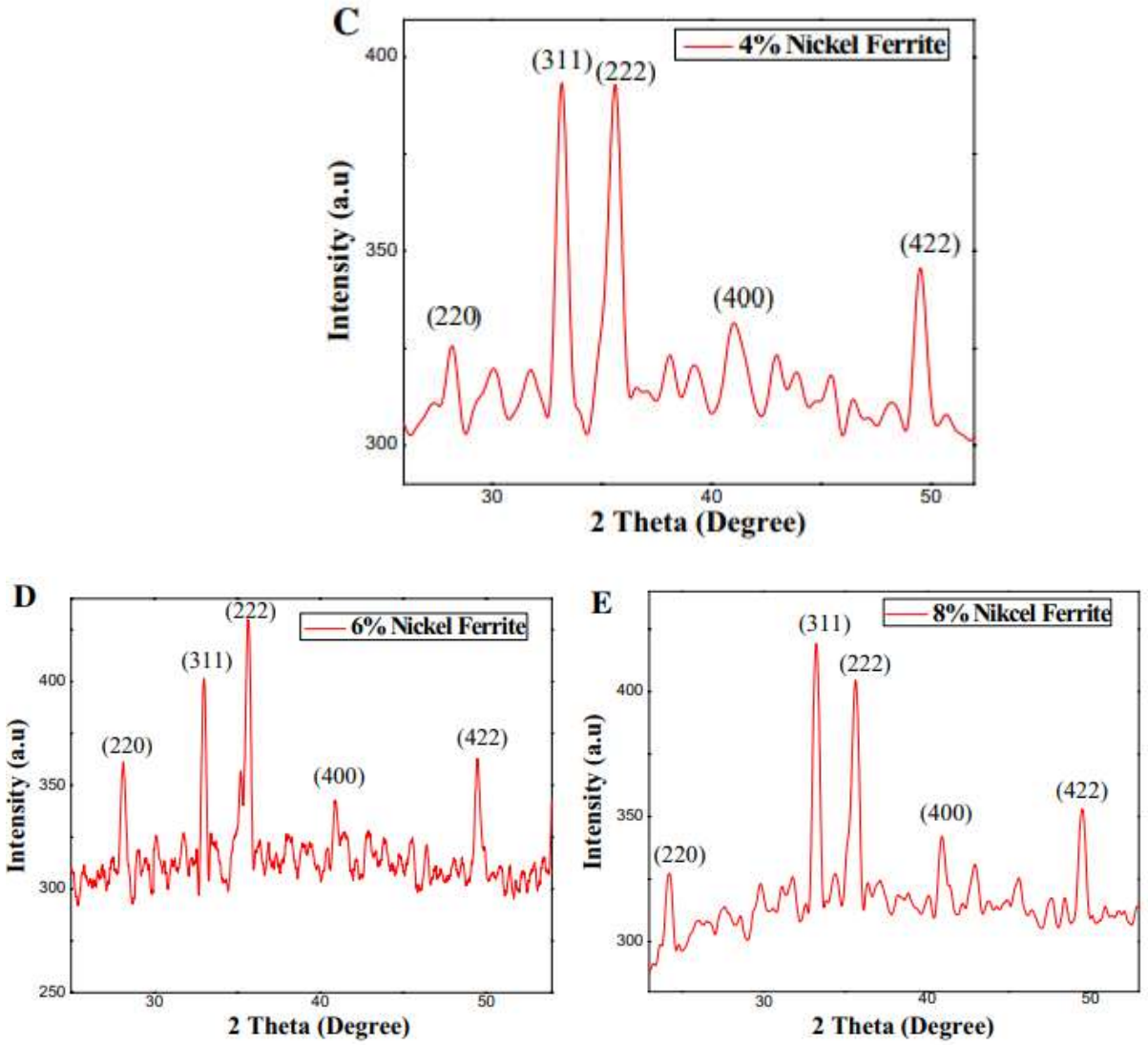

Fig. 4 X-ray diffraction analysis. a Pure ferrite, b 2%, c 4%, d 6%, e 8% nickel ferrite nanoparticles

In this particular instance, we investigate the transmittance of nanoparticles composed of pure ferrite and nickel ferrite. In the graphical explanation, the vertical axis represents the percentage of light that can pass through, and the horizontal axis represents the wavenumber of the infrared radiations. The range of wave number that has been decided upon is 400–4500 cm1, and the range of the percentage transmission along the vertical axis that has been decided upon is 50–100%.

Results and Discussion

Powder X-Ray Diffraction (XRD) Analysis

X-ray diffraction (XRD) is used to investigate the crystal structures of the magnetic particles. The information provided by the XRD is altered before being used to determine the miller indices of the crystal phases, which are then shown as peaks on the graph. The peaks that were seen.

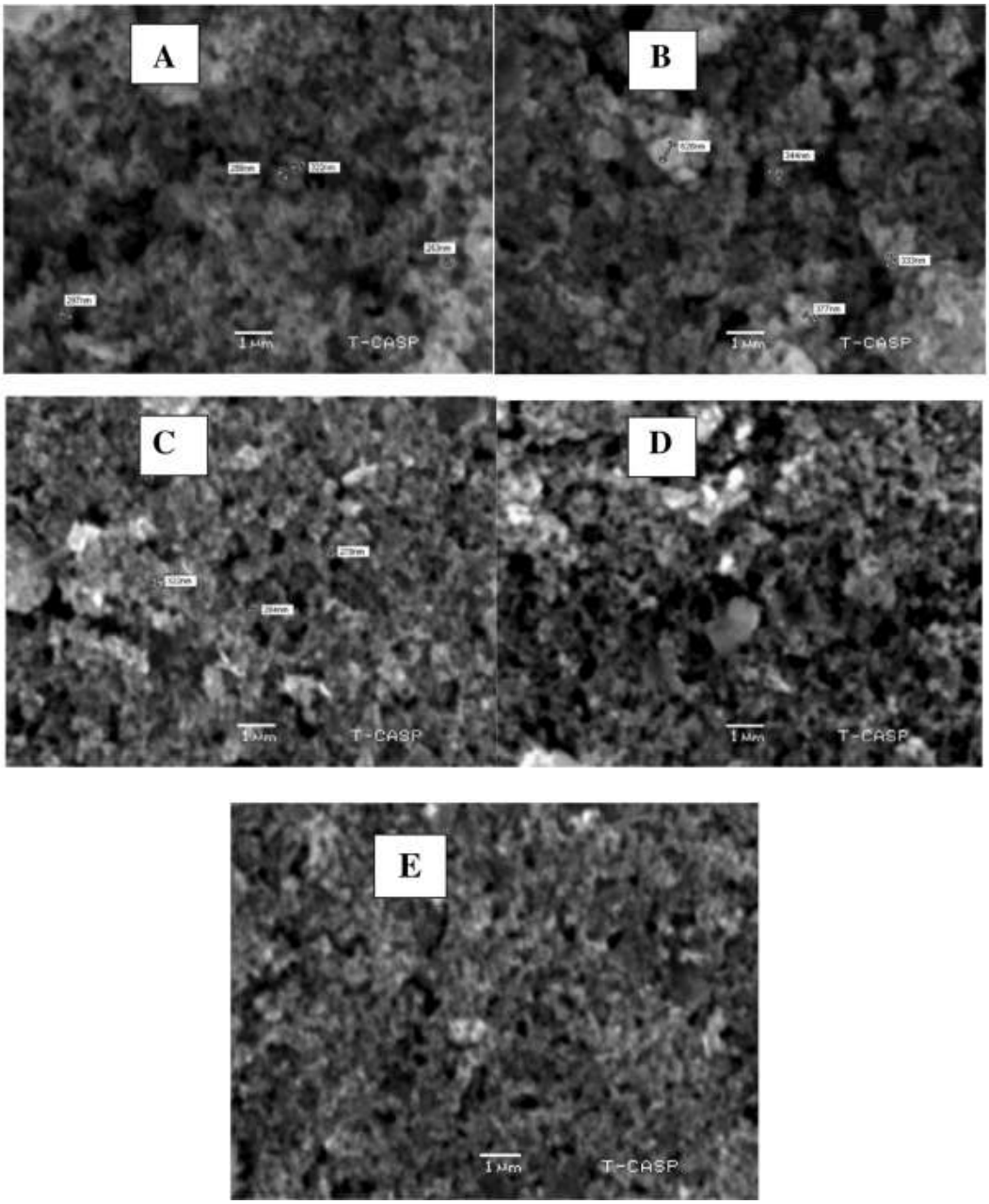

Fig. 5 SEM analysis of pure and nickel ferrite nanoparticles

using the XRD are compared with the Joint Committee Powder Diffraction Standards (JCPDS) data card No. 01-086-2267 for the identification of phase. This comparison revealed the phases (220), (311), (222), and (400), respectively (422). The XRD peaks of produced nanoparticles with varying concentrations of nickel are displayed in Figure 4. The miller indices are a particularly useful indicator for the presence of a spinal cubic structure in nickel ferrite nanoparticles. This structure has a lattice value of 8.393, which indicates the inclusion of other phases such as hematite Fe2O3 or nickel oxide. Because of the smaller range of values for the nickel content, the peaks on the graph have moved in the other direction. This demonstrates that the concentration of nickel in the nickel ferrite nanoparticles is proportional to the size of the nanoparticles. The nanoparticles of nickel ferrite are increasing in size, and the predicted particle size is increasing within the range of 40–60 nm.

Scanning Electron Microscope Analysis (SEM)

Figure 5 displays scans from a scanning electron microscope that were taken of nanoparticles that were manufactured using the wet chemical co-precipitation process and had varying amounts of nickel. Figures a, b, c, d, and e have been given the names pure ferrite, 2% nickel ferrite nanoparticles, 4% nickel ferrite nanoparticles, and 8% nickel ferrite nanoparticles accordingly. By using a scaling approach, the nickel ferrite nanoparticles have a size that falls between 250 and 400 nm and have a uniform morphological appearance with only a little degree of aggregation. The incorporation of nickel results in the production of nickel oxide as well as ferric oxide from ferric oxide, which in turn leads to an expansion of the grain size of the nickel ferrite nanoparticles. Because of this, the size of the grains is found to be related to the amount of nickel present.

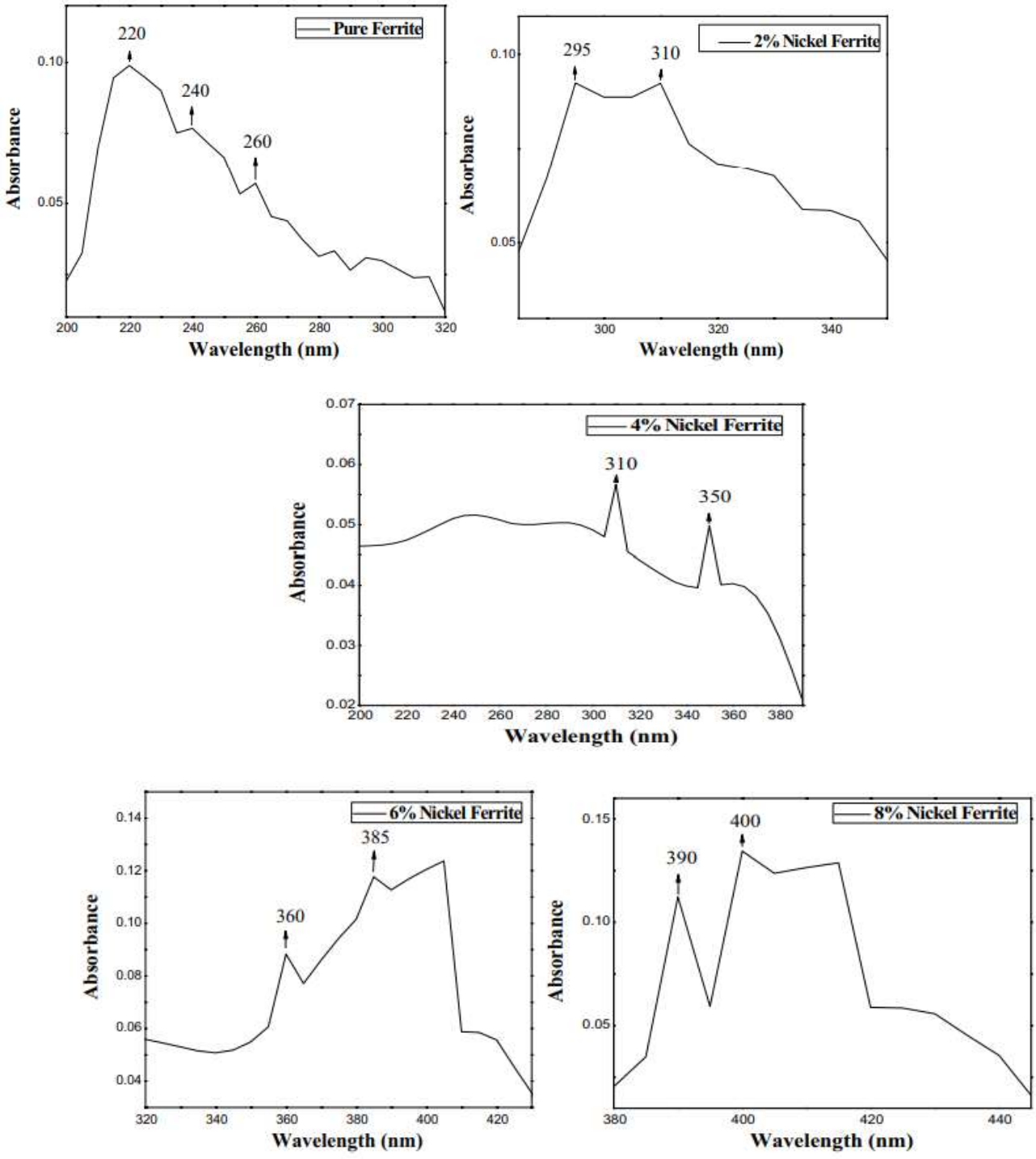

Fig. 6 UV–Vis spectrometry analysis of nickel ferrite with different concentrations

Ultra-Violet Visible Spectroscopy Analysis

Figure 6 presents the findings obtained from the UV–Vis characterization. The change in absorbance between pure nickel ferrite nanoparticles and nickel ferrite nanoparticles is represented graphically below. By increasing the percentage of nickel in ferrite, UV–Vis reveals a red shift within the range of absorption peaks that occurs between 200 and 400 nanometers. The band gape narrows as a result of red shift, which also results in an increase in particle size. Therefore, lowering the quantity of nickel will result in a smaller band gap for the atoms, while increasing the particle size.

Conclusion

Various amounts of nickel were used throughout the manufacturing process of the nickel ferrite nanoparticles. It should be pointed out that the characteristics of the finished products are reliant on the quantity of nickel that was included into the ferrite nanoparticles. According to the findings of XRD, the size of the nickel particles in ferrite grows larger as the concentration of nickel in the ferrite increases. It was also determined that the inclusion of nickel changed the crystal structure of the nickel ferrite nanoparticle from a face-centered cubic structure to a body-centered cubic structure. This was another finding that led to the conclusion. The FTIR analysis came to the conclusion that increasing the quantity of nickel causes a shift in the transmission peaks toward the front of the spectrum. It demonstrated a direct correlation between the amount of nickel and the transmission. The red shift of the light that is seen in the UV–Vis spectrum is a direct indicator of the inverse impact that has been having on the band gape. The scanning electron microscopy examination reveals a rise in the average particle size of nickel ferrite nanoparticles as a result of an increase in the nickel content. This study is useful for the fabrication of devices intended to store data, for the classification of inorganic materials, which play a very important role in the various aspects of life due to their outstanding magnetic, electronic, and optical properties, and for a variety of other applications as well.

References

1. M. Dariel, L.H. Bennett, D.S. Lashmore, J. Appl. Phys. 61, 4067 (1987)
2. W.D. Williams, N. Giordano, Phys. Rev. B 33, 8146 (1986)
3. T.M. Whitney, J.S. Jiang, P.C. Searson, Science 261, 1316 (1986)
4. L. Piraux, J.M. George, J.F. Despres, C. Leroy, Appl. Phys. Lett. 65, 2484 (1994)
5. J. Yang, S.B. Park, H.G. Yoon, Y.M. Huh, S. Haam, Int. J. Pharm. 324, 185–190 (2006)
6. F.X. Hu, K.G. Neoh, E.T. Kang, Biomaterials 27, 5725–5733 (2006)
7. Y.L. Luo, L.H. Fan, F. Xu, Y.S. Chen, C.H. Zhang, Q.B. Wei, Mater. Chem. Phys. 120, 590–597 (2010)
8. K.V.P.M. Shafi, Y. Koltypin et al., J. Phys. Chem. B 101, 6409 (1997)
9. M. Khaldi, A. Benyoucef, C. Quijada, A. Yahiaoui, E. Morallon, J. Inorg. Organomet. Polym. Mater. 24, 267–274 (2014)
10. Z. Cai, C.R. Martin, J. Am. Chem. Soc. 111, 4138 (1989)
11. S.K. Chakarvarti, J. Vetter, Nucl. Instrum. Methods Phys. Res. B 62, 109 (1991)
12. S.K. Chakarvarti, J. Vetter, J. Micromech. Microeng. 3, 57 (1993)

13. S. Larumbe, C.G. Polo, J.I.P. Landazábal, A.G. Prieto, J. Nanosci. Nanotechnol. 12, 1–9 (2012)
14. S. Benykhlef, A. Bekhoukh, R. Berenguer, E. Morallon, Colloid Polym. Sci. 294, 1877–1885 (2016)
15. I. Radja, H. Djelad, E. Morallon, A. Benyoucef, Synth. Met. 202, 25–32 (2015)
16. M. Kooti, A.N. Sedeh, J. Mater. Sci. Technol. 29, 34–38 (2013)